Application of a Three-Stage Procedure for Extracting a Small-Sized Anchor Object on a Noisy Image

Sotnikov O.M.[1], Vorobiov O.M.[2], Udovenko S.G.[3], Kobzev I.V.[3], Vlasiuk V.V.[4], Kurbatov A.A.[4]
[1]Kharkiv National University of the Air Force named after Ivan Kozhedub, Kharkiv, Ukraine.
[2]National University of Defense, Kyiv, Ukraine.
[3]Kharkiv National Economic University named after Semen Kuznets, Kharkiv, Ukraine.
[4]Kyiv Institute of the National Guard of Ukraine, Kyiv, Ukraine.

Abstract. The purpose of the article is to develop a three-stage procedure for identifying an anchor object in a noisy current image. This goal is achieved by determining the sampling threshold levels at which the greatest similarity of the compared images is ensured; development of a procedure for refining the maximum of the decision function by quantizing the current image. The solution to the first problem is based on the formation of a correlation field of radio brightness temperatures and the choice of a sampling threshold. It is proposed to use the cross-correlation coefficient as a criterion for the degree of image matching. The effectiveness of the procedure for selecting a fragment of a reference image is assessed based on the criterion of the probability of selecting a fragment of a reference image. It is shown that image noise can lead to a decrease in the probability of selecting a fragment of a reference image, down to 0.4. It is proposed to refine the maximum of the decision function based on the iteration method. The most significant results are the obtained dependences of the probability of choosing a fragment of the reference image on the threshold value and the signal-to-noise ratio, as well as the analytical relation for the asymptote of this dependence. The novelty of the work lies in the fact that the procedure for forming the decisive function has been further developed. This will significantly improve the operating efficiency of unmanned aerial vehicles, especially in conditions of interference.
Keywords: unmanned aerial vehicle, three-stage procedure for forming the decision function, image discretization and quantization, probability of choosing a fragment of the reference image.
DOI: https://doi.org/10.52254/1857-0070.2024.1-61.08
UDC: 62-758.381

Aplicarea unei proceduri în trei etape pentru identificarea unui obiect ancora de dimensiune mică într-o imagine zgomotoasă

Sotnikov O.M.[1], Vorobiov O.M.[2], Udovenko S.G.[3], Kobzev I.V.[3], Vlasiuk V.V.[4], Kurbatov A.A.[4]
[1] Universitatea Națională a Forțelor Aeriene din Harkiv, numită după Ivan Kozhedub, Harkiv, Ucraina
[2] Universitatea Națională de Apărare a Ucrainei, Kiev, Ucraina
[3] Simon Kuznets Harkiv Universitatea Națională de Economie, Harkiv, Ucraina
[4] Kiev Institutul Gărzii Naționale a Ucrainei, Kiev, Ucraina

Rezumat. Scopul articolului este de a elabora o procedură în trei etape pentru identificarea unui obiect ancora într-o imagine curentă zgomotoasă. Acest obiectiv este atins prin determinarea nivelurilor pragului de eșantionare la care se asigură cea mai mare similitudine a imaginilor comparate; elaborarea unei proceduri de rafinare a maximului funcției de decizie prin cuantificarea imaginii curente. Soluția primei probleme se bazează pe formarea unui câmp de corelare a temperaturilor de luminozitate radio și alegerea unui prag de eșantionare. Se propune utilizarea coeficientului de corelație încrucișată ca criteriu pentru gradul de potrivire a imaginii. Eficacitatea procedurii de selectare a unui fragment dintr-o imagine de referință este evaluată pe baza criteriului probabilității de selectare a unui fragment dintr-o imagine de referință. Se arată că zgomotul de imagine poate duce la o scădere a probabilității de selectare a unui fragment dintr-o imagine de referință, până la 0,4. Se propune rafinarea maximului funcției de decizie pe baza metodei de iterație, în funcție de numărul de elemente obiect din imagine și de numărul de emisii laterale ale funcției de decizie. Cele mai importante rezultate sunt dependențele obținute ale probabilității de alegere a unui fragment din imaginea de referință de valoarea pragului și raportul semnal-zgomot, precum și relația analitică pentru asimptota acestei dependențe. Noutatea lucrării constă în faptul că procedura în trei etape pentru prelucrarea secundară și formarea funcției decisive a fost dezvoltată în continuare. Acest lucru va îmbunătăți semnificativ eficiența operațională a vehiculelor aeriene fără pilot, în special în condiții de interferență.
Cuvinte cheie: vehicul aerian fără pilot, procedură în trei etape pentru generarea unei funcții de decizie, eșantionare și cuantificare a imaginii, probabilitate de selectare a unui fragment dintr-o imagine de referință.

Применение трехэтапной процедуры выделения малоразмерного объекта привязки на зашумленном изображении

Сотников А.М.[1], Воробьев О.М[2]., Удовенко С.Г[3]., Кобзев И.В[3]., Власюк В.В[4]., Курбатов А.А[4].
[1]Харьковский национальный университет Воздушных Сил имени Ивана Кожедуба, Харьков, Украина
[2]Национальный университет обороны, Киев, Украина
[3]Харьковский национальный экономический университет имени Семена Кузнеца, Харьков, Украина
[4] Киевский институт Национальной гвардии Украины, Киев, Украина

Аннотация. Целью статьи является разработка трехэтапной процедуры выделения малоразмерного объекта привязки на текущем изображении, формируемом радиометрической системой технического зрения в условиях воздействия помех. Поставленная цель достигается определением величины уровней порога дискретизации, при которых обеспечивается наибольшее сходство фрагмента эталонного изображения с текущим изображением; оценкой эффективности процедуры выбора эталонного изображения с учетом помеховой обстановки; разработкой процедуры уточнения максимума решающей функции путем квантования текущего изображения в зависимости от числа элементов, при которых достигается максимум решающей функции. Решение первой задачи основано на формировании корреляционного поля радиояркостных температур и выборе порога дискретизации, при котором обеспечивается наибольшее совпадение искомого фрагмента эталонного изображения с текущим. В качестве критерия степени совпадения изображений предложено использовать коэффициент взаимной корреляции. Оценена эффективность процедуры выбора фрагмента эталонного изображения по критерию вероятности правильного выбора фрагмента эталонного изображения из набора с учетом помеховой обстановки и величины относительного порога. Показано, что зашумление изображений может приводить к значительному снижению эффективности процедуры выбора фрагмента эталонного изображения, вплоть до 0.4. На третьем этапе поиск максимума решающей функции предложено осуществлять на основе метода итерации для двух вариантов в зависимости от количества элементов объекта на изображении и числа боковых выбросов решающей функции. Наиболее существенным результатом являются полученные зависимости вероятности правильного выбора искомого фрагмента эталонного изображения от величины порога и отношения сигнал-шум изображения, а также аналитическое соотношение для асимптоты этой зависимости. Новизна работы заключается в том, что получила дальнейшее развитие трехэтапная процедура вторичной обработки и формирования решающей функции в системах технического зрения с использованием набора эталонных изображений. Это позволит существенно повысить эффективность функционирования беспилотных летательных аппарата, особенно в условиях воздействия помех.

Ключевые слова: беспилотный летательный аппарат, трехэтапная процедура формирования решающей функции, дискретизация и квантование изображений, вероятность выбора фрагмента эталонного изображения.

INTRODUCTION

Currently, there is a significant surge in the use of unmanned aviation technologies across various industries, agriculture, emergency response, and particularly in monitoring hard-to-reach areas, especially during military conflicts. In autonomous UAVs operating at considerable distances, navigation is facilitated through satellite navigation systems such as NAVSTAR (USA), GLONASS (Russia), BEIDOU (China), and others [1]. Additionally, systems implementing the panoramic-comparative navigation method [2] are also employed. The latter belong to the class of correlation-extremal navigation systems (CENS). The accuracy characteristics of these systems are primarily determined by the degree of correspondence between frames of current images (CI) generated by information extraction sensors and the reference image (RI). The result of image correspondence depends on errors in determining the spatial coordinates of UAVs, the formation of RI, and the orientation of information extraction sensors. The positional accuracy error of UAVs when using CENS can reach 35…45 m in coordinates, 6…13 m in height, and 0.1…0.2º in positioning angles [3]. At altitudes of around 100 m, the error can be of the order of 1 radian, whereas the required image comparison errors should not exceed 5 mrad horizontally and vertically. It is necessary to generate 105…106 perspectives of the reference image (RI) per second, which, in the case of implementing exhaustive comparison of all possible perspectives of the current image (CI), exceeds the performance of classical computing architecture by at least a factor of 103. In [4], it is demonstrated that using the method of exhaustive comparison of all possible perspectives of RI and CI in a six-dimensional space (latitude, longitude, height, roll, yaw, pitch) to solve the problem of finding the global maximum of the decision function (DF) through real-time image

comparison is not feasible. It is noted that with 10 discrete values per coordinate and 5 per angle, exhaustive enumeration would require N=125,000 perspectives of RI. Achieving such a quantity of alignments in real-time at the current technological level is challenging. In [5], an approach is proposed to enhance the performance of the computer vision system (CVS) by iteratively selecting from a set of reference images (RI) the one most closely resembling the current image (CI). The accuracy characteristics of the CVS using this approach are solely determined by the degree of correspondence of the selected RI fragment with the CI, which will be influenced by the discretization intervals of the RI in terms of navigation parameters and angular orientation parameters. Consequently, there arises a need to organize another iterative process that ensures a more precise selection of the reference object using an adaptive algorithm. To achieve this, quantization of the CI based on the values of an informative parameter must be performed. This stage becomes significantly important when locating the UAV on the navigation route with the presence of small-sized objects, especially under the influence of interference leading to a reduction in the signal-to-noise ratio in the image, which, in turn, deteriorates the accuracy characteristics of the CVS. Various applications of multipath processing for the purpose of selecting an object of interest on the current image (CI) have been explored in numerous works [6-11]. Multipath processing is based on the properties of the intensity histogram of the original image. The final stage of the segmentation process involves the selection of a threshold value, which may not be optimal since each object may require its own threshold value depending on its characteristics. In a series of articles [12-16], authored in further development, algorithms for extracting and localizing small-scale objects are proposed based on preliminary filtering, threshold processing, and morphological selection. The suggested multipath processing algorithm is implemented using a multi-channel construction of the processing system, predetermining the use of specific threshold values with subsequent determination of the most suitable one. As such, no iterative adaptation to the threshold is presented. This approach is akin in essence to the one discussed in [5]. The distinction lies in using binary slices of CI instead of a set of reference images (RI), with each slice assigned its own processing channel. In [17], an algorithm for forming a unimodal decision function (DF) for the radiometric computer vision system (CVS) is proposed. The algorithm involves preprocessing the current image (CI), which consists of dividing it into layers relative to the mean value of radiometric brightness temperature of the background and determining the set of objects with the highest radiometric brightness temperature. The fragment of the CI layer with the set of objects with the highest radiometric brightness temperature is then used to form the DF. Effectively, representing the CI as a certain number of slices also constitutes multipath processing with the establishment of a threshold relative to which the task of determining the DF is solved. The procedure for searching for an adaptive threshold is not utilized. In [18], the formation of the DF is suggested to be based on using large-sized reference images (RI), which would eliminate the need for exhaustive enumeration of values in terms of yaw. According to the authors, this would lead to a reduction in the computational complexity of image alignment. To eliminate enumeration along roll and pitch angles, using the horizon line or non-correlational alignment along roll is proposed. Non-correlational alignment along roll is based on finding the real horizon line and aligning it with the synthesized one. However, due to the low flight altitude and the changing nature of the flight trajectory, such an approach is impractical for UAVs. In [19], the results of applying a genetic algorithm in combined computer vision systems are presented. To search for the global extremum, it is suggested to use expanded angles of the reference image (RI). It is noted that this increases the performance of the secondary processing system by a factor of 5. However, the authors did not consider the influence of the increased angles of the RI, and consequently, the possible perspectives of the RI, on the real-time process of forming the decision function (DF). In [20], the research results on forming the DF when aligning the CVS in conditions of creating the current image (CI) with a non-stationary structure are presented. The modeling results confirmed the effectiveness of the proposed methods for generating CI and DF by radiometric systems. At the same time, the authors overlooked the impact of the interference environment on the selection of the reference object and the need to search for the global maximum of the DF. In [21-24], issues of object contour detection and localization on images using the Hough transform are discussed, considering the impact of scale distortions on the object localization process on the current image

(CI). The results of optimizing the object detection procedure on images are presented. However, these studies do not account for the influence of the interference environment on determining the global maximum of the DF. Additionally, they do not consider constraints on the computational complexity of image alignment. In [25], the results of statistical studies on an adaptive image comparison algorithm are presented, and general approaches to organizing the iterative process of selecting the desired object are formulated. In [30-31], adaptive algorithms for image processing and segmentation, as well as accuracy assessments of determining the motion parameters of an aerial target under covert observation, are proposed based on the application of the iteration method. However, the authors did not propose any specific implementation of an adaptive image comparison algorithm, and they did not take into account the characteristics of the formed decision function (DF) in terms of the number of lateral outliers and the number of elements at which the maximum of the DF is achieved. Thus, despite the significant attention from researchers towards the development of methods and algorithms for UAV navigation, there is a need for further advancement, especially in challenging conditions of interference and complex background-object scenarios. In this context, the implementation of methods and algorithms for forming the decision function (DF) in computer vision systems (CVS) should consider the stages and peculiarities of DF formation based on the principles of building the secondary processing system of the CVS. For instance, the use of a set of reference images (RI) for forming the DF leads to a three-stage procedure for finding the global maximum of the DF. The first two stages are aimed at searching for the relevant RI fragment from the available set to form the DF, considering navigation parameters and then angular orientation parameters. In the third stage, quantization of the already formed current image (CI) is assumed to search for the global maximum of the DF. Thus, searching for the global maximum of the DF involves initially searching for the RI fragment from the available set, followed by an iterative search to refine the DF maximum, ensuring precise determination of the AO's coordinates on the CI. Therefore, DF formation should be based on a three-stage procedure, including the determination of the RI fragment most corresponding to the CI based on defining threshold values for the RI discretization in terms of an informative parameter, evaluating the effectiveness of the threshold selection procedure for the RI, and developing an iterative procedure to refine the DF maximum through quantization of the formed CVS CI, including noisy ones, considering possible decision-making scenarios regarding the number of lateral outliers of the DF and the number of CI elements at which the DF reaches its maximum.

The aim of the article is to develop a three-stage procedure for detecting a small-sized Anchor Object (AO) on the current image (CI) generated by a computer vision system (CVS), taking into account its noise. To achieve this goal, the following tasks needed to be addressed:

- Determine the threshold discretization levels at which the fragment of the reference image (RI) exhibits the highest similarity with the CI.
- Evaluate the effectiveness of the RI selection procedure.
- Develop a procedure for refining the decision function (DF) maximum through quantization of the formed CI, including noisy ones, considering possible scenarios for making a single decision based on the number of lateral outliers of the DF and the number of CI elements at which the DF reaches its maximum.

METHODS, RESULTS, AND DISCUSSION

1. Determination of the threshold discretization levels at which the fragment of the reference image (RI) exhibits the highest similarity with the current image (CI).

In general, the procedure for detecting an anchor object on the CI does not depend on the sensor type and, consequently, on the type of a measured informative parameter. Therefore, without loss of generality, let's consider the process of detecting an AO on the CI generated by a radiometric (RM) sensor in the computer vision system (CVS). In this case, the informative parameter is the radiometric temperature of objects and backgrounds.

Problem Statement.

The main task addressed by the radiometric Computer Vision System (CVS) at each stage of UAV trajectory referencing is to estimate the coordinates of a characteristic point of the selected reference object, denoted as $(x_{оп}, y_{оп})$, based on the processing of the radiometric relief $T(x,y)$ within the field of view $S \in R^2$. This involves utilizing prior information in the form of a Reference Image (RI) of one of the fragments within the CVS field of view, i.e., the creation of a mapping $S \to (x_{оп}, y_{оп})$.

This task breaks down into several subtasks:

1) Surveying the underlying surface in the area of the Anchor Object (AO).

2) Generating the radiometric relief of the terrain within the field of view of the Computer Vision System (CVS), i.e., creating a radiometric image (RMI).

3) Analyzing the RMI to detect anomalies caused by the presence of the AO, based on its comparison with the Reference Image (RI). Determining the coordinates of the characteristic point of the identified anomaly and providing target guidance to the UAV control system.

Let's assume that in the coordinate system (x, y) on the line of sight, the field of radiometric relief $T(x, y)$ is defined. A multi-beam antenna performs the transformation of radiometric radiation with intensity $T(x, y)$ into a set of processes $u_{T_{ij}}(t)_{i=1,j=1}^{N_1, N_2}$ with two-sided spectral power densities [2]:

$$S_{s_{ij}}(f) = kT(i, j)/2,$$

where the antenna temperature $T_{CI_{i,j}}$ is determined by the expression [2]:

$$T_{CI_{i,j}} = \int_{-\infty}^{\infty} \int_{-\infty}^{\infty} T(x, y) G(x_{ij} - x, y_{ij} - y) dx dy,$$

where $i \in \overline{1, N_1}$, $j \in \overline{1, N_2}$;

$G(x_{ij} - x, y_{ij} - y)$ is a function describing the i, j-th partial directional pattern of the antenna (DPA), recalculated to the coordinate system whose axis intersects the line of sight at point $(x_{OП}, y_{OП})$.

Thus, the distribution of the radiometric relief undergoes information loss due to discretization and quantization of the image, resulting from the finite number of processing channels and the "blurring" of the image due to the finite width of each partial DPA. This leads to a reduction in the accuracy of the CVS binding. The set of output signals from the radiometric channels forms the $N_1 \times N_2$ matrix of the CI $\boldsymbol{T}_{CI}$. Based on the comparison of fragments of this matrix with the reference matrix:

$$\boldsymbol{T}_{RI} = \left\| e_{ij} \right\|, \quad i \in \overline{1, M_1}, \; j \in \overline{1, M_2},$$

$$M_1 < N_1, M_1 < N_1$$

the secondary processing device, using an appropriate algorithm, makes a decision on the selection of the AO by searching for a CI fragment that most closely corresponds to the RI.

Current Image (CI) Model.

Let's use the "object on background" model of the CI, which is a zone model [26]. An object here refers to an entity or a combination of entities located in the field of view of the RM sensor, exhibiting stable radiometric contrast compared to the surrounding background. Thus, the CI represents a set of radiometric temperature values corresponding to objects and backgrounds in the resolution elements:

$$\boldsymbol{T}_{CI} = \left\| T(i, j) \right\|, \qquad (1)$$

where at

$$T(i, j) = \begin{cases} T_v(i, j), & \text{при } T(i, j) \in \boldsymbol{T}_v \\ T_w(i, j), & \text{при } T(i, j) \in \boldsymbol{T}_w \end{cases}$$

$T_v(i, j)$ - the brightness of the image element of the v-th object;

$T_w(i, j)$ - the brightness of the image element of the w-th background;

V and W - the number of objects and backgrounds in the frame, respectively.

Let's denote the contrast of the sought object relative to the surrounding background as $\Delta T(i, j) = T_v(i, j) - T_w(i, j)$. Then, the brightness distribution densities of the background and the object are determined by the expressions [4]:

$$w_w(T) = \frac{1}{\sqrt{2\pi}\sigma} exp\left[-\left(T - T_w\right)^2 / 2\sigma^2 \right], \qquad (2)$$

$$w_v(T) = \frac{1}{\sqrt{2\pi}\sigma} exp\left[-\left(T + T_v\right)^2 / 2\sigma^2 \right]. \qquad (3)$$

Let's represent by K_0 the number of cells in the frame with signals from a similar object; then

$$K_0 = K_v + K_w + K_\rho, \qquad (4)$$

where K_0 is the total number of frame elements within the line of sight;

K_v, K_w are the numbers of frame elements occupied by the anchor object and the background, respectively;

K_ρ is the number of frame elements distorted by interference signals.

For the CI model, we will make the following assumptions:

1) The CI has a size of $N_1 \times N_2$ pixels.

2) The values of the radiometric temperature of objects within the resolution element are homogeneous and exceed the radiometric temperature of the background.

3) The elements of the CI are normally distributed variables with a variance of σ_{ij}^2 and a mean value of $T(i,j)$, which, in the absence of interference, takes one of two values: $T_v(i,j)$ or $T_w(i,j)$ [27].

Reference Image (RI) Model.

Similar to CI, the RI has a zonal structure and is binary, with a size of $M_1 \times M_2$ pixels.

We will define the RI, assuming its configuration is known, as follows. Place an RI with K_v elements on the CI matrix. Then, consider the element with the smallest number in the vector representation of CI as the reference element of the object.

The task of selecting the object involves determining the number of the reference element, based on which the coordinates of the reference element in the matrix representation can be found [25]:

$$i_{op} = div_{N_2} c_{op} + 1,\ j_{op} = \mathrm{mod}_{N_2} c_{op}. \qquad (7)$$

Noise Model.

Let's assume that part of the image elements, denoted as K_p, may be distorted by signals from two types of spatial noise. The first type includes active noise with a positive temperature contrast relative to the background. Signals from the first type of noise can be filtered and excluded from the frame before processing by narrowing the dynamic range of the receiver. The second type of noise includes signals from unstable formations, for example, water accumulations (pools) after precipitation. In accordance with the principle of the CVS operation, for comparing CI with individual fragments of RI and determining the closest fragment as a measure of similarity, we will use the coefficient of cross-correlation (CCC) $K_{max}(i,j,\Delta h)$. For each (i,j), the CCC is determined according to the expression [2]:

$$K_{ij}(k,l,\Delta h) = \frac{1}{N_1 N_2} \sum_{m=1}^{N_1} \sum_{n=1}^{N_2} T_{CI_{ij}}(m,n) \times T_{RI}(m+k-1, n+l-1, \Delta h), \qquad (8)$$

$$\mathbf{K}_{ij} = \left\| K_{ij}(k,l,\Delta h) \right\|, \qquad (9)$$

when $k = 1...M_1 - N_1$, $l = 1...M_2 - N_2$,

where Δh is the change in UAV height.

For each matrix $\mathbf{K}_{ij}$, its maximum value is determined:

$$K_{max}(i,j,\Delta h) = \max_{kl} \left\| K_{ij}(k,l,\Delta h) \right\|, \qquad (10)$$

where $i = 1...M_1 - N_1$, $j = 1...M_2 - N_2$;

$T_{RI_{ij}}(m,n) \in T_{CI}$ and $T_{RI}(m+k-1, n+l-1, \Delta h) \in T_{CI}$.

Matrix (10), with a size of $(M_1 - N_1) \times (M_2 - N_2)$, characterizes the distribution $K_{max}(i,j,\Delta h)$ and represents the correlation field of radiometric temperatures (CFRT). The process of forming CFRT can be represented by the relation:

$$K_{ij}(k,l,\Delta h) = \frac{1}{N_1 N_2} \sum_{m=1}^{N_1} \sum_{n=1}^{N_2} [T_{RI_{ij}}(m,n) - \bar{T}_{RI_{ij}}] \times [T_{CI}(m+k-1, n+l-1, \Delta h) - \bar{T}_{CI_{kl}}] \qquad (11)$$

To determine the RI fragment that best matches CI, it is advisable to apply L threshold levels:

$$K_1 < K_{KIPT} \le K_2,\ K_2 < K_{KIPT} \le K_3, \ldots,$$

$$K_L < K_{KIPT} \le 1, \qquad (12)$$

where $K_1 = K_{nop}$.

Since it is necessary to select an RI fragment from the set, the use of which should provide the maximum value of the CCC, threshold levels for which the condition $K_{KIPT} \le 0.5$ is satisfied can be excluded from consideration. By choosing threshold level values within $0.5 < K_{KIPT} \le 1$, it is possible to identify the most suitable RI fragment for forming the CVS DF. Let's illustrate this with an example. Choose a threshold level change step equal to 0.1. Use selective images obtained for different CCC values ($K_{ij} = 0.6...0.9$), as shown in Fig. 1-4.

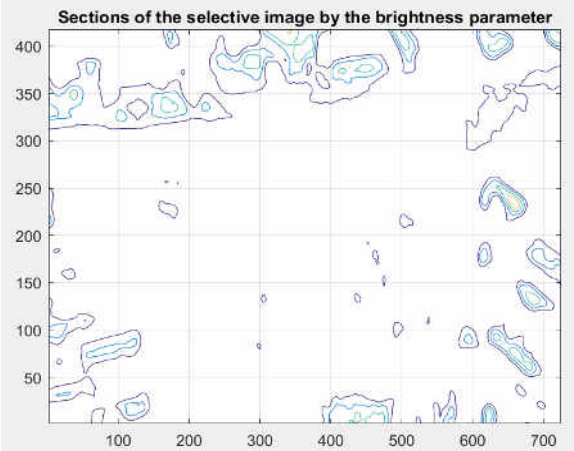

Fig. 1. Selective imaging of the correlation field of radio brightness temperatures (BRBT) ($K_{ij} = 0.6$).

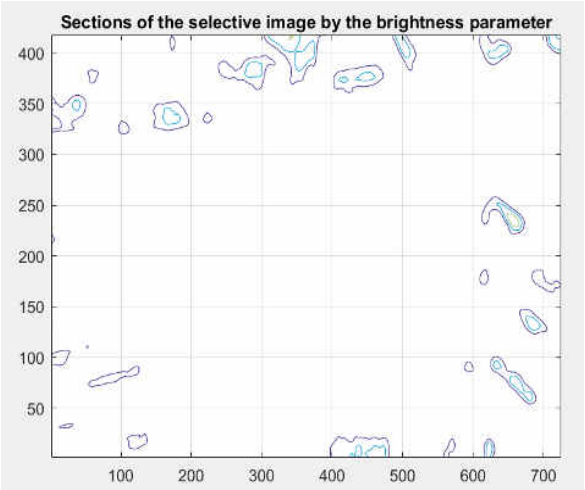

Fig. 2. Selective imaging of the correlation field of BRBT ($K_{ij} = 0.7$).

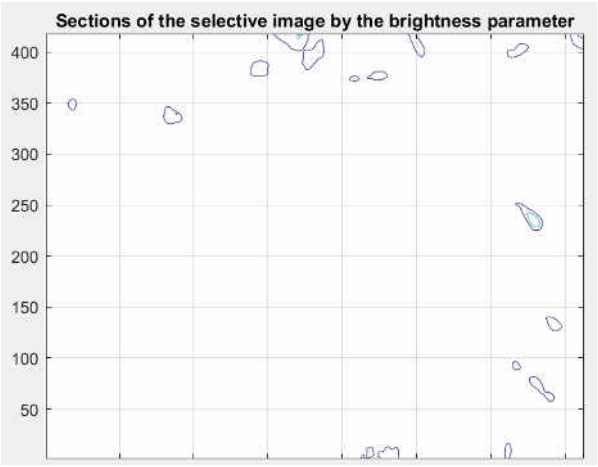

Fig. 3. Selective imaging of the correlation field of BRBT ($K_{ij} = 0.8$).

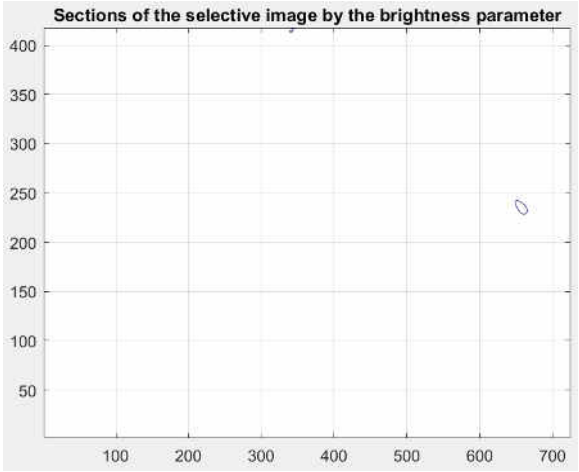

Fig. 4. Selective imaging of the correlation field of BRBT ($K_{ij} = 0.9$).

In Figures 5 and 6, the results of constructing the CFRT corresponding to the images shown in Figs. 1 and 4 are presented.

The simulation results demonstrate that by choosing threshold levels of discretization at the first and second stages of forming the DF, it is possible to ensure the correct identification of the RI fragment from the available set. This is confirmed by the unimodality of the function shown in Figure 6. The maximum CCC (Fig. 6) corresponds to a small-sized object in an image with developed infrastructure, having a significant number of objects close in size but with lower radiometric temperature, as clearly seen in Fig. 3.

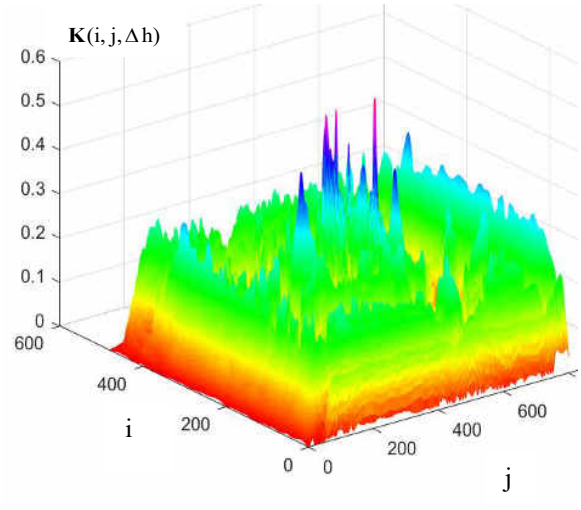

Fig. 5. The correlation field of radio brightness temperature, constructed for the selective image shown in Fig. 1.

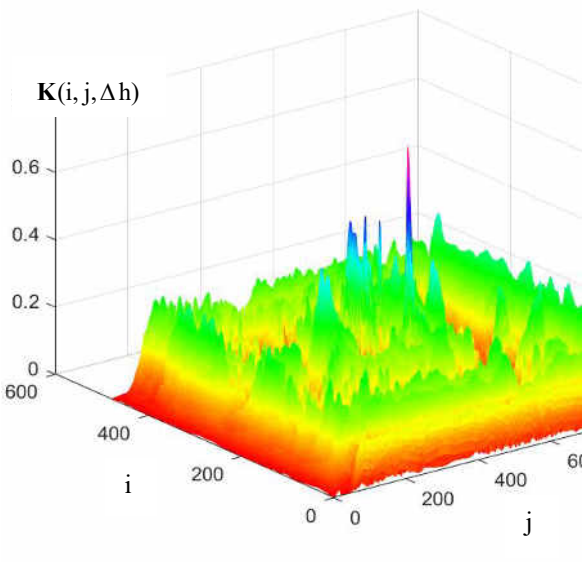

Fig. 6. The correlation field of radio brightness temperature, constructed for the selective image shown in Fig. 4.

The presented results of the threshold level selection research were conducted without considering the influence of noise and image contamination, which necessitates the evaluation of the effectiveness of the proposed approach in practical applications.

2. Evaluation of the effectiveness of the multi-threshold procedure for selecting RI.

Problem Statement.

Let's assume that the DF formation procedure does not involve a third stage of DF maximum refinement. In other words, the CVS is designed so that the AO coordinates are estimated based on the comparison results of the generated CI and a selected fragment of the RI, using threshold levels of discretization. Since the procedure for selecting the RI fragment from the available set is similar to the multi-threshold procedure for detecting the AO on the CI, we will assess the effectiveness based on the probability of correctly choosing the RI fragment from the set P_B. To quantitatively assess the desired probability, we will use an analytical relationship provided in [26] with the adopted notations:

$$P_B = \sum_{j=1}^{K_v} C_{K_v}^{j} \left(1-\alpha\right)^{j} \alpha^{K_v-j} \times \times \left[\sum_{k=0}^{j-1} C_{K_v}^{k} \beta^{k} \left(1-\beta\right)^{K_v-k}\right]^{K}, \quad (13)$$

where

$$\alpha = \alpha(l') = \int_{T_F \cdot l}^{\infty} w_v(T)dT = 1-\Phi\ q-l' , \quad (14)$$

$$\beta = \beta(l') = \frac{1}{1+T}\left[\Phi(-l') + Te^{-\lambda' l'}\right], \quad (15)$$

α, β - errors of the first and second kind, respectively;

Φ - probability integral;

$l' = l/\sigma$ - relative threshold;

$\lambda' = \lambda\sigma$.

The results of numerical calculations P_B are presented in Figs. 7 and 8.

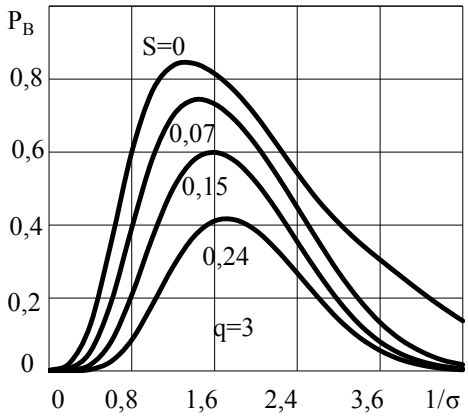

Fig. 7. Dependence of the probability of correct selection of an RI fragment on the value of the relative threshold.

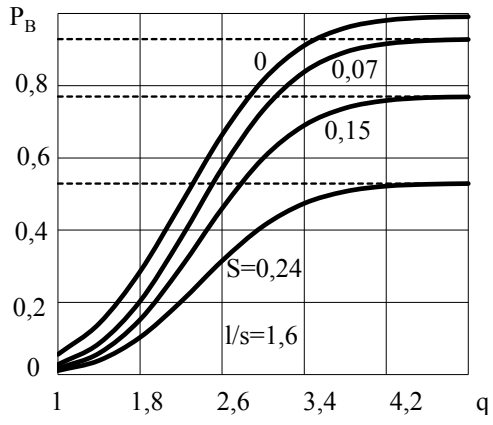

Fig. 8. Dependence of the probability of correct choice of the binding object on the signal-to-noise ratio.

Calculations were performed for typical signal-to-noise ratio values of radiometric channels, taking into account possible noise in the CI.

The influence of noise on the CI is considered

through various values of the interference parameter $S = K_\rho / K_v$. The signal-to-noise ratio $q = \Delta T/\sigma$ is chosen in the range from 1 to 5.

For the selected initial data, dependencies of the probability of correctly choosing the RI fragment most corresponding to the CI on the relative threshold value l' were obtained for the chosen interference conditions.

Each curve in the family has a horizontal asymptote at $q \to \infty$. To find the equation of the asymptote, we use the asymptotic representation of the probability integral [28]:

$$\Phi(x) \approx 1 - \sqrt{\frac{2}{\pi}} \frac{e^{-x^2/2}}{x},\ x \to \infty .$$

Then, according to expression (14), we write:

$$\alpha(q) \approx \sqrt{\frac{2}{\pi}} \frac{e^{-q^2/2}}{q},\ q \to \infty , \qquad (16)$$

And the probability β according to (15) does not depend on the signal-to-noise ratio q. Since from expression (16) it follows that $\alpha(q) \to 0$ at $q \to \infty$, then in the sum over j, the predominant value is the term with $j = K_v$. Therefore, the equation of the asymptote of the function $P_B(q)$ takes the form:

$$P_B = \left[\sum_{k=0}^{j-1} C_{K_v}^k \beta^k \left(1 - \beta\right)^{K_v - k} \right]^K . \qquad (17)$$

The asymptotes of the curves $P_B(q)$ for different values of the interference environment factor are shown by dashed lines in Fig. 8. Analysis of the curves $P_B(q)$ suggests that increasing the signal-to-noise ratio of the image above five is impractical, as it does not provide a gain in probability P_B. At the same time, it is necessary to note that the deterioration of the interference environment, leading to image noise, significantly affects P_B, which can lead to a considerable reduction, even below 0.4. This means that to determine the CVS coordinates of the AO, it is necessary to refine the maximum DF by performing the third stage of the iterative procedure for finding the maximum DF, including the noisy one, taking into account possible decision options for the number of sidelobes in the DF and the number of CI elements at which the maximum DF is reached.

3. Results of a detailed development of the iterative procedure for refining the maximum DF, taking into account possible decision options.

It is known that any iterative procedure involves performing work in parallel with continuous analysis of the obtained results and adjusting subsequent stages of work. In a general sense, the organization of the iterative process concerning the analysis and refinement of the maximum DF is presented in [25]. However, the authors did not propose implementation options for the iterative procedure, and possible situations were not considered, both in terms of the number of objects and the number of sidelobes in the DF. This necessitates a detailed development of the iterative procedure for finding a unique solution.

Solution to the problem.

Let's use the vector representation of the CI in the form of the unfolding of the matrix by rows [25]:

$$\boldsymbol{T}^v = \left(T_1^v, \ldots, T_{N_{im}}^v\right)\ \left(N_{im} = N_1 N_2\right). \qquad (18)$$

Consider one of the possible options for the iterative search for the maximum DF.

First, calculate the estimate of the mean value of the radiometric temperature of the background $\hat{T}_w$. Then, according to the iteration method [29], choose the initial threshold value $l^0 = \alpha\sigma$ (algorithm trials have shown that it is advisable to choose $\alpha \in 1{,}8 \ldots 2{,}2$), relative to which the CI will be transformed into a binary image denoted by H^0. Then, by comparing the obtained CI with the selected fragment of the RI, we will construct the decision function matrix $\left\| R_{i,j}^0 \right\|$ and find the set of elements K^0 at which the maximum DF is achieved, using the expression:

$$K^0 = \left\{ (k,l) \in \overline{1, N_1} \times \overline{1, N_2} \left(R_{kl} = \max_{i,j} R_{ij} \right) \right\} . \qquad (19)$$

The maximum of the decision function $R_{\max}^0$ is not necessarily equal to K_v, it is possible that $R_{\max}^0 < K_v$.

If the set K^0 consists of a single element, i.e., $K^0 = \{(k,l)\}$, the decision is made that the coordinates of the anchor object relative to the CI are k, l. Otherwise, an iterative process is organized, involving the change of the initial threshold value l^0 to l^1, the formation of a new binary image H^1 relative to the threshold l^1, the calculation of the decision function matrix $\left\| R_{i,j}^1 \right\|$

for the image H^1, and the calculation of the set K^1. To organize the iterative process, it is necessary to determine the iteration step size and its sign. In the considered algorithm with an adaptive threshold regime, it is proposed to make a decision under the condition that, on some i-th iteration, the set K^i consists of a single element, and $R^i_{\max} = K_v$. Hence, if the maximum of the DF is not unique and is equal to K_v, it is necessary to choose $\Delta l_1 = l^1 - l^0 > 0$. Otherwise, the iteration should have a negative sign. The selection of the step for each iteration should be carried out in such a way that, on the next i-th iteration, the binary image H^i differs from H^{i-1} but differs insignificantly.

It is advisable to use the following method. Unroll the matrix of the CI $\|T(i,j)\|$ by rows and denote by $\{T_i\}_{i=1}^{N_{ti}}$ ($N_{ti} = N_1 N_2$) the sequence of elements of the CI, ranked in ascending order.

Consider two possible cases:

1) Suppose the set K^0 contains more than one element, and $R^0_{\max} = K_v$ is present at the initial threshold value l^0. Then for some $j \in \overline{1, N_{ti}}$, the inequality $T_{j-1} \le \hat{T}_w - l^0 < T_j$ holds. Set the step Δl_1 according to the condition $\Delta l_1 = \hat{T}_w - T_{j-1} - l^0$. Then the threshold becomes $l^1 = l^0 + \Delta l_1 = \hat{T}_w - T_{j-1}$, and in the binary image H^1, compared to H^0, the one corresponding to the element $T_j \in \{T_i\}_{i=1}^{N_{ti}}$ disappears.

If the set K^1 contains more than one element and $R^1_{\max} = K_v$, then a threshold $l^2 = \hat{T}_w - T_{j-2}$ is chosen, and the iteration process continues until either at some k-th iteration, the set K^k contains a single element and $R^k_{\max} = K_v$, or K^k contains multiple elements and $R^k_{\max} = K_v - 1$. In the first case, the solution is accepted based on the position of the sole maximum, and in the second case, a decision to reject the solution is made. The situation corresponding to the second case arises when the removed one from the binary image H^{k-1}, corresponding to the element $T_k \in \{T_i\}_{i=1}^{N_{ti}}$, is common to several image fragments H^{k-1}, consisting of ones and having the configuration of an anchor object.

2) Let K^0 be a set with more than one element and $R^k_{\max} < K_v$. Define the iteration step as follows: $\Delta l_1 = \hat{T}_w - T_{j+1} - l^0$. Then, the threshold $l^1 = \hat{T}_w - T_{j+1}$ is determined, and on the binary image H^1, a one appears corresponding to the element $T_{j+1} \in \{T_i\}_{i=1}^{Nti}$. The iterative process continues until at some m-th iteration, $R^m_{\max} = K_v$. occurs. If the set K^m contains a single element, a decision is made to select the anchor object based on the coordinates of this element; otherwise, a decision to reject is made. Obviously, the iterative procedure for determining the coordinates of the AO will have a higher probability of selecting the AO on the CI. However, obtaining an analytical expression for estimating the probability of selecting an object on the CI proved to be quite difficult, unlike the multipath algorithm, which necessitates the use of modeling.

CONCLUSIONS

As a result of the conducted research, a three-stage procedure for detecting a small-sized Anchor Object (AO) on a noisy image has been developed. The influence of the discretization threshold levels on the similarity between the Reference Image (RI) fragment and the Current Image (CI) has been demonstrated. It has been established that to detect a small-sized AO on the CI with a large number of objects close in size to the AO, it is necessary to choose the discretization threshold $K_{ij} = 0.9$. The efficiency of the procedure for selecting the RI based on the discretization threshold level, taking into account the noise environment, has been evaluated. It has been found that the probability of selecting an RI fragment from the existing set depends largely on image noise and may decrease to 0.4, necessitating the refinement of the Decision Function (DF) maximum. A detailed procedure for determining the DF maximum based on the iteration method has been proposed. This procedure essentially represents an algorithm for refining the DF maximum through CI quantization depending on the number of elements at which its maximum is achieved.

References

[1] Kadem R.K. Komponentnyi Analiz Bezpilotnykh Lital′nykh Aparativ. // Elektronika ta Systemy Upravlinnya. - 2010. - № 2 (24). - pp. 45-51. (In Russian).

[2] Sotnikov O., Kartashov V., Tymochko O., Sergiyenko O., Tyrsa V., Mercorelli P., Flores-Fuentes W. Methods for Ensuring the Accuracy of Radiometric and Optoelectronic Navigation Systems of Flying Robots in a Developed Infrastructure (eds) Machine Vision and Navigation. Springer, Cham. https://doi.org/10.1007/978-3-030-22587-2_16.

[3] Kostyashkin, L.M. Problemni Aspekty Systemy Kombinovanoho Bachennya lital′nykh Aparativ [Tekst]/L.M. Kostyashkin, A.A. Lohinov, M.B. Nykyforov// Yzvestyya YUFU. – 2013. – №5. – pp. 61-65. (In Russian).

[4] Elesina S., Lomteva O. Increase in Image Combination Performance in Combined Vision Systems Using Genetic Algorithm // Proceedings of the 3rd Mediterranean Conference on Embedded Computing. – Budva, Montenegro.– 2014. pp. 158-161.

[5] Yeromina, N., Tarshyn, V., Petrov, S., Salo, N., Chumak, O. Method of Reference Image Selection to Provide High-Speed Aircraft Navigation under Conditions of Rapid Change of Flight Trajectory. International Journal of Advanced Technology and Engineering Exploration, Vol. 8(85), pp. 1621- 1638. DOI:10.19101/IJATEE.2021.874814.

[6] Gonsales R., Vudc R., Eddins S. Tsifrovaya Obrabotka Izobrazhenii v Srede MATLAB. M.: Tekhnosfera, 2006. 615 p.

[7] Pakhomov A.A. Obrabotka Iskazhenii Atmosferoy Izobrazheniy, Poluchennykh Aviatsionnymi Kompleksami [Tekst] / A.A. Pakhomov, A.A. Potapov // Uspekhi Sovremennoy Radioelektroniki. – Radiotekhnika – 2015. – №5. – pp. 144-145. (In Russian).

[8] Fernandes, L. Real-Time Line Detection through an Improved Hough Transform Voting Scheme [Text] / Leonardo A.F. Fernandes, Manuel M. Oliveira // Pattern Recognition. – 2008. – V. 41, N 1. – pp. 299-314. – ISSN 0031-3203.

[9] Fursov, V. A. Lokalizatsiya Konturov Ob"yektov na Izobrazheniyakh pri Variatsiyakh Masshtaba s Ispol'zovaniyem Preobrazovaniya Khafa [Tekst] / V. A. Fursov, S. A. Bibikov, P. YU. Yakimov // Komp'yuternaya Optika.– 2013. – T. 37, № 4. – pp. 496-502.

[10] Maji, S. A Max-Margin Hough Transform for Object Detection [Text] / S. Maji, J. Malik. // Proc. of IEEE Computer Society Conference on Computer Vision and Pattern Recognition. – 2009.

[11] Katulev, A. N. Adaptivnyi Metod i Algoritm Obnaruzheniya Malokontrastnykh Ob"yektov Optiko-Elektronnym Sredstvom [Tekst] / A. N. Katulev, A. A. Kolonskov, A. A. Khramichev, S. V. Yagol'nikov // Opticheskiy Zhurnal. – 2014. – № 2(81). – pp. 29-39.

[12] Volkov V. Yu., Turnets′kyy L.S. Porohova Obrobka dlya Sehmentatsiyi ta Vydilennya Protyazhnykh Ob'yektiv na tsyfrovykh zobrazhennyakh // Informatsiyno-keruyuchi systemy. 2009. № 5 (42). pp. 10-13. (In Russian).

[13] Volkov V. Yu. Adaptive Identification of Small Objects in Digital Images // Izv. universities in Russia. Radioelectronics. 2017. № 1. pp. 17–28. (In Russian).

[14] Volkov V. Yu. Detecting Objects in Images Using Area Selection. Issues of Radio Electronics. 2020. №. 2. pp. 6-11. (In Russian).

[15] Volkov V. Yu. Adaptive and Invariant Algorithms for Detecting Objects in Images and their Modeling in Matlab. 2014. pp.192-192. (In Russian).

[16] Volkov, V. Yu., Markelov, O. A., & Bogachev, M. I. (2019). Image Segmentation and Object Selection Based on Multi-Threshold Processing. News of Higher Educational Institutions of Russia. Radioelectronics, 22, №3, pp. 24-35. (In Russian).

[17] N.Yeromina, S. Petrov, A. Tantsiura, M. Iasechko, V. Larin. Formation of Reference Images and Decision Function in Radiometric Correlation-Extremal Navigation Systems. Eastern-European Journal of Enterprise Technologies. — 2018. Vol. 4, No.9 (94). — pp. 27—35. DOI: 10.15587/1729-4061.2018.139723.

[18] Elesina S., Lomteva O. Increase in Image Combination Performance in Combined Vision Systems Using Genetic Algorithm // Proceedings of the 3rd Mediterranean Conference on Embedded Computing. – Budva, Montenegro. – 2014. pp. 158-161.

[19] Tymochko O., Ttystan A., Ushan V., Yeromina N., Dmitriiev O., Mazharov V., Padalka I., Hannoshyna I., Masik I., Zazirnyi A. The Synthesis of the Reference Image and Algorithms for Vehicle Navigation Systems, IJETER, 8(3), 2020, pp. 853-858. doi:10.30534/ijeter/2020/40832020.

[20] Yeromina N., Kurban V., Mykus S., Peredrii O., Voloshchenko O., Kosenko V., Kuzavkov V., Babeliuk O., Derevianko M., Kovalov H. The Creation of the Database for Mobile Robots Navigation under the Conditions of Flexible Change of Flight Assignment. International Journal of Emerging Technology and Advanced Engineering, 2021, 11(5), pp. 37–44. doi.org/10.46338/ijetae 0521_05.

[21] Yeromina N., Petrov S., Tantsiura A., Iasechko M., Larin V. Formation of Reference Images and Decision Function in Radiometric Correlation-Extremal Navigation Systems, Eastern-European Journal of Enterprise Technologies. — 2018. Vol.4, No.9 (94). — pp. 27—35. DOI: 10.15587/1729-4061.2018.139723.

[22] Yeromina N., Petrov S., Antonenko N., Vlasov I., Kostrytsia V., Korshenko V. The Synthesis of the Optimal Reference Image Using Nominal and Hyperordinal Scales, IJETER, 8 (5), 2020, pp. 2080-2084, doi:10.30534/ijeter/2020/98852020.

[23] Liashko O., Klindukhova V., Yeromina N., Karadobrii T., Bairamova O., Dorosheva A. The Criterion and Evaluation of Effectiveness of Image Comparison in Correlation-Extreme Navigation Systems of Mobile Robots, IJETER, 8 (6), 2020, pp. 2841-2847, doi:10.30534/ijeter/2020/ 97862020.

[24] Yeromina N., Samoilenko V., Chukanivskyi D., Zadkova O., Brodova O., Levchenko O. The Method of Iterative Formation of Selective Reference Images, IJETER, 8 (7), 2020, pp. 3753-

3759, doi:10.30534/ijeter/2020/ 138872020.
[25] Yeromina N., Petrov S., Samsonov Y., Pisarevskiy S., Kaplun S., Vlasenko I. The Simulation and Performance Evaluation of Adaptive Algorithm of Image Comparison in Correlation-Extreme Navigation Systems, IJETER, 8 (8), 2020, pp. 4146-4151, doi:10.30534/ijeter/2020/19882020.
[26] Dzhayn A.K. Uspikhy v Haluzi Matematychnykh Modeley dlya Obrobky Zobrazhen′ // TIIER. – 1981. – T. 69, №5. – pp. 9-39.
[27] Methods for Filtering Signals in Correlation-Extremal Navigation Systems / V.K. Baklitsky, A.M. Bochkarev, M.P. Musyakov. - M.: Sov. radio, 1986. - 216 p.
[28] Janke E., Emde F., Lesh F. Special Functions: Trans. with him. - M.: Nauka, 1977. - 344 p.
[29] Demidovich B.P. and Maron I.A. Fundamentals of Computational Mathematics. – M. Nauka, 1970. – 664 p.
[30] Chentsov, A. A., Chentsov, A. G., & Chentsov, P. A. (2009). Iteration Method in a Routing Problem with Internal Cosses. Proceedings of the Institute of Mathematics and Mechanics, Ural Branch of the Russian Academy of Sciences, 15(4), pp. 270-289. (In Russian).
[31] Gurov, I. P., Sizikov, V. S., & Shchekotin, D. S. (2003). Methods for Image Reconstruction in X-ray Tomography. Scientific and Technical Bulletin of Information Technologies, Mechanics and Optics, (11), pp. 97-104. (In Russian).

Information about authors.

Sotnikov Oleksandr Mykhailovych, Doctor of Technical Sciences, Professor principal scientist, Kharkov National Air Force University; area of scientific interests: Navigation systems for mobile robots, image processing methods and algorithms,
E-mail: alexsot@ukr.net.
ORCID: https://orcid.org/0000-0001-7303-0401

Vorobiov Oleh Mykhailovych, Doctor of Technical Sciences, Professor, Professor of the rear support department of the National Defense University of Ukraine. Area of interest: intelligent systems digital data processing.
E-mail: oleg33377@ukr.net.
ORCID: https://orcid.org/ 0000-0001-5362-1976

Udovenko Sergey Grigorievich Doctor of Technical Science, Professor, Head of Department Simon Kuznets Kharkiv National University of Economics.
Area of interest: intelligent systems digital data processing.
E-mail: serhiy.udovenko@hneu.net ,
ORCID: https://orcid.org/0000-0001-5945-8647

Kobzev Igor Volodymyrovych Candidate of Technical Sciences. Associated professor Department of informatics and computer technique Simon Kuznets Kharkiv National University of Economics. Area of interest: intelligent systems digital data processing.
E-mail: ikobzev12@gmail.com, http://orcid.org/0000-0002-7182-5814

Vlasiuk Valerii Vasilievich Head of the Department of Tactics and Tactical Special Training of the Kyiv Institute of the National Guard of Ukraine. Area of scientific interests: navigation.
E-mail: vlasyukvv1986@gmail.com.
ORCID: https://orcid.org/0000-0002-2140-3250

Kurbatov Artem Andreevich Lecturer at the Department of Tactics and Tactical Special Training of the Kyiv Institute of the National Guard of Ukraine. Area of scientific interests: navigation.
E-mail: kurbatov57@icloud.com.
ORCID: https://orcid.org/0000-0003-1674-9588